JOURNAL OF SOLID STATE CHEMISTRY 105, 336–345 (1993)

Temperature Dependence of the Structure of $Li_{1-x}H_xIO_3$ Studied by High Resolution Neutron Powder Diffraction between 10 and 380 K

J.-M. CRETTEZ* AND E. COQUET

Université de Bourgogne, Faculté des Sciences et Techniques, Laboratoire OSC: Ondes et Structures Cohérentes, 6 Boulevard Gabriel, 21000 Dijon Cedex, France

J. BOUILLOT AND J. LE ROY

Université de Savoie, Institut Universitaire de Technologie, Laboratoire Structure de la Matière, 9 rue de l'Arc en Ciel, B.P. 240, 74942 Annecy Le Vieux Cedex, France

AND J. PANNETIER

Institut Laue–Langevin, 156X, 38042 Grenoble Cedex, France

Received May 11, 1992; in revised form November 18, 1992; accepted November 23, 1992

Thermal variations of structural parameters of $Li_{1-x}H_xIO_3$ are reported between 10 and 380 K, and are compared to isotypic α-$LiIO_3$ in the same temperature range. Beside the presence of a weakly bound, randomly distributed proton in general position of $P6_3$, differences appear concerning the thermal expansion coefficient along the polar axis and a significant shift of the Li position is observed from 210 K to the decomposition temperature ($\approx$400 K). This predicts differences in the $Li_{1-x}H_xIO_3$ pyroelectric and piezoelectric effects when compared to the α-$LiIO_3$ crystal widely used for technological applications.

Introduction

The lithium iodate crystal α-$LiIO_3$ (space group $P6_3$) is widely used in applied physics owing to its striking nonlinear, photoelastic, piezoelectric, and pyroelectric properties. Among noncentrosymmetric iodates, lithium iodate–iodic acid solid solutions $Li_{1-x}H_xIO_3$, first mentioned by Ricci and Amron (*1*), have been recognized as prospective materials for technical applications, in particular owing to the largest piezoelectric d_{33} coefficient within the series of iodates (*2*) when the HIO_3 content x (mole fraction) takes the value 0.30. Unlike α-$LiIO_3$, only a few results have been published about the solid solution, probably because of difficulties in obtaining large homogeneous (relative to H^+ content) single crystals suitable for applications. From a preliminary study by neutron thermodiffractometry (*3*), the thermal behavior of a $Li_{1-x}H_xIO_3$ powder above room temperature (RT) appeared to be more complex than that of α-$LiIO_3$. Whereas the latter is stable up to 500 K (the temperature of the $\alpha \rightarrow \gamma$ and $\gamma \rightarrow \beta$ phase transitions depending on the morphology, the growth conditions, and the mechanical and thermal history of the sample (*4*)), the solid solution is found to be stable from RT to only 398 K. Above this temperature, the H^+ concentration decreases, then new compounds (among which are α-$LiIO_3$, HI_3O_8, and H_2O) appear in the sequence of transformation–decomposition, and finally a mix-

* To whom correspondence should be addressed.

0022-4596/93 $5.00

ture of tetragonal β-$LiIO_3$ and I_2O_5 is obtained at 560 K. In spite of a relatively low transformation temperature and difficulties in obtaining large single crystals, the study of the thermal behavior of the $Li_{1-x}H_xIO_3$ structure is of fundamental interest since this compound has been recently found to be isotypic with α-$LiIO_3$ at RT (*5*). Indeed, the knowledge of the structural temperature dependence of $Li_{1-x}H_xIO_3$ could be useful in understanding some properties of hexagonal lithium iodate related to the pH of the growth solution that are particularly sensitive to the H^+ impurity concentration, such as dc ionic conductivity and anomalous dielectric behavior at low frequency (*6*).

In $Li_{.67}H_{.33}IO_3$, our X-ray single crystal and neutron powder diffraction structure refinements at RT have shown that the Li and IO_3 network is kept and that the hydrogen atoms do not occupy the position of lithium atoms in their sites (2a in Wyckoff notation) but are randomly distributed in general position (6c sites) with an occupation factor 0.33. Hydrogen is weakly bounded to the two nearest oxygens, which allows the pyramidal IO_3 groups not to be distorted. The analysis of crystallization products obtained from aqueous solutions of $LiIO_3$ containing various amount of HIO_3 shows that $Li_{1-x}H_xIO_3$ forms as a single phase only within the limits $0.22 \leq x \leq 0.36$. The reasons for these particular values of the limiting compositions are not yet understood.

The aim of our investigation, undertaken by means of high-resolution neutron powder diffraction, was first to complete the thermal study of $Li_{1-x}H_xIO_3$ below RT in order to determine the whole domain of stability and second to investigate the possible splitting of hydrogen sites.

Experimental and Data Collection

The sample used in this experiment was a finely ground powder of hexagonal rods of $Li_{1-x}H_xIO_3$ obtained by slow isothermal evaporation ($T \approx 303$ K) of an aqueous solution containing $LiIO_3$ and HIO_3 in the correct stoichiometry (*7*). At RT the *c*/*a* ratio of unit cell dimensions varies linearly with the H^+ content (*5*). From the calculated value of this ratio at RT, the x value for the sample was established to be 0.34 within an accuracy of 5%. The neutron diffraction patterns were recorded on the D2B high-resolution high-flux powder diffractometer at the Institut Laue–Langevin in Grenoble. The sample was enclosed in a cylindrical vanadium container (10 mm in diameter) and mounted in a cryofurnace. Data were collected at a wavelength $\lambda = 1.5945$ Å in the angular range $2\theta = 5°$ to 160° in steps of 0.025°. Measurement time was about 30 sec per step. At a given temperature the data of the 64 counters spaced at 2.5° intervals were summed using a conventional ILL program. The sample was first cooled to 10 K at a rate of 2 K min^{-1}. Following the recording of the diffraction pattern during 8 h at 10 K, the temperature was raised with regular steps of 50 K up to 310 K. The pattern was also recorded at two higher temperatures, 350 and 380 K, the latter being 18 K below the expected beginning of the transformation.

Structure Refinements

The diffraction patterns were analyzed by the Rietveld method using the Wiles and Young profile refinement program (*8*). A pseudo-Voigt function was chosen to generate the line shape of the diffraction peaks and the background was fitted as a third order polynomial simultaneously with other instrumental and structural parameters. The neutron scattering lengths were $b(Li) = -0.1900$, $b(H) = -0.3740$, $b(I) = 0.5280$, and $b(O) = 0.5805$ fm. As far as absorption is concerned, two contributions have to be considered: Li gives rise to a classical absorption which can be accounted using a coefficient $\sigma(Li) = 63 \times 10^{-24}$ cm^2 and H causes an absorption resulting from its incoherent scattering and which can be evaluated using a coefficient $\sigma(H) = 80 \times 10^{-24}$ cm^2. From these values, a coefficient $\mu =$

1.13 cm^{-1} can be calculated. A direct measurement of the sample absorption gives $\mu = 0.56$ cm^{-1}, which is coherent with the theoretical value which does not consider the partial filling of the container by the powder. If such an absorption, which corresponds in this case to $\mu r = 0.28$ (r is the sample holder radius), is not taken into account, it will result an underestimation of overall Debye–Waller factor B of 0.05 which in our refinements is within the error (*9*). Asymmetry corrections were applied for angles less than 40°. Excluding the upper and lower zones of the patterns, 121 *hkl* reflexions corresponding to 68 independent observed intensities were taken into account in the range $16° < 2\theta < 159°$. Starting with the atomic coordinates previously obtained by X-ray single crystal refinement at RT (*5*) and holding occupation factors fixed at values determined by the stoichiometry of the sample, refinements were carried out in space group $P6_3$. The Li, I, and O atoms were allowed to vibrate anisotropically while the temperature factor of H was refined as isotropic. After a few cycles, refinements converged with reliability factors R_N and R_p in the ranges 3.4% to 5.7% and 3.7% to 4.2% respectively. A typical plot is reported in Fig. 1 which shows the agreement between the observed and calculated profiles at 10 K.

Results and Discussion

Assuming the location of hydrogen in a single site (general position of the space group), nine sets of structural parameters were obtained from refinements at different temperatures. Parameters and estimated standard deviations (esd's) are reported in Tables I and II.

From 10 to 380 K the background of the diffraction patterns increases slightly and lattice parameters vary regularly without any anomaly, which indicates no decomposition of the sample. Indeed, neutron powder thermodiffractometry experiments (*3*) have shown that the first step of transformation, which has been interpreted as the release of protons out of the lattice, consists in a decrease of the background and drastic variations of cell parameters in opposite direction (a decreases whereas c increases).

Lattice Parameters and Thermal Expansivity

The nine sets of hexagonal lattice constants a and c were fitted by polynomial regression analysis and yield the following results expressed in terms of $\Delta T = (T - 295)$ K:

$$a(\Delta T) = 5.5634\,(1 + 20.2 \times 10^{-6}\,\Delta T + 9.19 \times 10^{-9}\,\Delta T^2 - 58.7 \times 10^{-12}\,\Delta T^3)\ (\text{Å})$$

$$c(\Delta T) = 4.9538\,(1 + 70.5 \times 10^{-6}\,\Delta T + 111 \times 10^{-9}\,\Delta T^2 - 8.7 \times 10^{-12}\,\Delta T^3)\ (\text{Å}).$$

The principal thermal expansion coefficients derived from these polynomials are

$$\alpha_a(\Delta T) = 20.2 \times 10^{-6}\,(1 + 0.89 \times 10^{-3}\,\Delta T - 8.7 \times 10^{-6}\,\Delta T^2)\ (\text{K}^{-1})$$

$$\alpha_c(\Delta T) = 70.5 \times 10^{-6}\,(1 + 3.1 \times 10^{-3}\,\Delta T - 0.69 \times 10^{-6}\,\Delta T^2)\ (\text{K}^{-1}).$$

These expressions give a better description of the thermal expansivity than the constant coefficients $\alpha_a \approx 18 \times 10^{-6}$ K^{-1}, $\alpha_c \approx 80 \times 10^{-6}$ K^{-1} obtained from the low resolution neutron thermodiffractometry experiments performed on the D1B diffractometer (*3*). The variations of α_a and α_c vs temperature are plotted in Fig. 2. Owing to the small coefficient of ΔT^2 in $\alpha_c(\Delta T)$, originating from an almost parabolic shape of $c(\Delta T)$, the α_c parameter exhibits a quasi linear variation with temperature. For comparison, the coefficients of pure α-$LiIO_3$ in the same temperature range (*10*) are also reported in Fig. 2. The thermal expansion coefficients of $Li_{1-x}H_xIO_3$ are of the same order of magnitude as those of α-$LiIO_3$ from 10 K up to about 150 K but differ at higher temperatures, especially along the polar axis. At 380 K, $\alpha_c(Li_{1-x}H_xIO_3) = 86.6 \times 10^{-6}$ K^{-1} while $\alpha_c\ (LiIO_3) = 52.5 \times 10^{-6}$ K^{-1}. Nevertheless the volume expansion coefficient (the sum

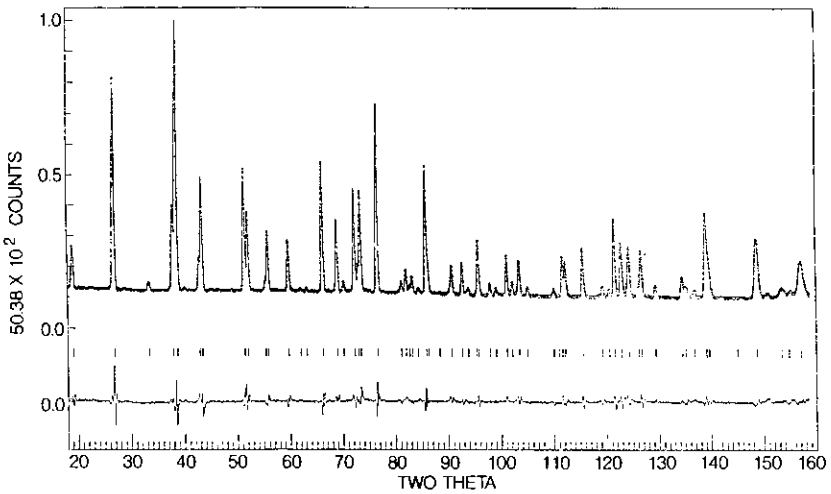

FIG. 1. Neutron diffraction profile of $Li_{1-x}H_xIO_3$ at 10 K. Crosses are the raw data points; the solid line is the best fit profile. The difference plot (observed − calculated) appears at the bottom. The tick marks below the profile indicate the positions of allowed reflections included in the calculation.

TABLE I

LATTICE PARAMETERS AND REDUCED ATOMIC COORDINATES IN $Li_{1-x}H_xIO_3$ FROM HIGH RESOLUTION NEUTRON POWDER DIFFRACTION

	Temperature (K)								
T	10	60	110	160	210	260	310	350	380
	Lattice parameters (Å)								
a	5.54294(4)	5.54411(4)	5.54647(4)	5.54984(4)	5.55434(4)	5.55946(4)	5.56541(4)	5.56981(5)	5.57293(5)
c	4.90019(7)	4.90243(7)	4.90795(7)	4.91642(7)	4.92896(7)	4.9435(7)	4.95688(8)	4.97479(9)	4.98821(9)
	Lithium ($\times 10^3$)								
z	−43(3)	−47(3)	−49(3)	−44(3)	−41(3)	−52(3)	−57(4)	−63(4)	−57(5)
	Hydrogen ($\times 10^3$)								
x	293(3)	293(3)	290(3)	284(3)	288(3)	293(3)	293(3)	286(4)	283(4)
y	53(3)	53(3)	51(3)	53(3)	53(3)	58(3)	63(3)	48(4)	45(4)
z	−532(2)	−530(2)	−532(3)	−537(2)	−537(2)	−541(2)	−547(2)	−541(3)	−540(3)
	Oxygen ($\times 10^4$)								
x	3529(2)	3529(2)	3530(2)	3533(2)	3535(2)	3536(2)	3536(2)	3540(2)	3539(2)
y	2654(1)	2653(1)	2650(2)	2649(2)	2648(2)	2644(2)	2639(2)	2642(2)	2640(2)
z	1780(4)	1776(4)	1766(4)	1753(5)	1746(5)	1743(5)	1741(5)	1732(6)	1719(6)
	Reliability factors (%)								
R_N	3.53	3.42	3.87	4.18	4.30	4.07	5.17	5.51	5.66
R_p	4.17	3.98	4.00	4.08	4.06	3.72	3.83	3.99	3.90

Note. Li is at (0, 0, z), I at ($\frac{2}{3}$, $\frac{1}{3}$, 0), O and H at (x, y, z) in $P6_3$. The occupancies of Li and H are fixed to 0.66 and 0.34 respectively. The reliability factors "R-nuclear" and "R-profile" are reported at the bottom of the table.

TABLE II

ANISOTROPIC THERMAL PARAMETERS ASSOCIATED TO Li, I, O ATOMS GIVEN IN TABLE I IN $Li_{1-x}H_xIO_3$ FROM HIGH RESOLUTION NEUTRON POWDER DIFFRACTION

	Temperature (K)								
T	10	60	110	160	210	260	310	350	380
				Lithium ($\times 10^3$)					
β_{11}	8(1)	9(1)	8(1)	8(1)	9(1)	8(1)	11(1)	16(2)	19(2)
β_{33}	47(2)	48(2)	52(2)	60(2)	61(3)	67(3)	78(3)	82(4)	91(4)
				Hydrogen (Å^2)					
B_{iso}	1.57(18)	1.55(17)	1.54(18)	1.35(18)	1.50(18)	1.55(18)	2.27(23)	2.99(30)	3.71(34)
				Iodine ($\times 10^4$)					
β_{11}	64(5)	74(5)	85(5)	104(5)	121(6)	135(5)	152(6)	169(6)	178(7)
β_{33}	177(3)	185(3)	199(3)	227(4)	221(4)	222(3)	233(4)	261(4)	271(4)
				Oxygen ($\times 10^4$)					
β_{11}	64(2)	77(2)	86(2)	98(2)	118(3)	138(3)	154(3)	179(3)	196(4)
β_{22}	120(3)	132(3)	149(3)	176(4)	205(4)	230(4)	253(4)	287(5)	313(6)
β_{33}	277(2)	285(2)	298(2)	317(2)	340(2)	361(2)	385(2)	413(2)	422(2)
β_{12}	41(3)	49(3)	56(3)	69(3)	80(3)	91(3)	99(3)	117(4)	130(4)
β_{13}	51(6)	50(6)	44(6)	38(7)	53(7)	49(7)	40(7)	49(8)	52(8)
β_{23}	−15(5)	−13(5)	−20(5)	−25(6)	−27(6)	−30(6)	−35(6)	−34(7)	−33(7)

Note. The temperature factor of H is isotropic; the general anisotropic temperature factor expression is $\exp[-(\beta_{11}h^2 + \beta_{22}k^2 + \beta_{33}l^2 + 2\beta_{12}hk + 2\beta_{13}hl + 2\beta_{23}kl)]$.

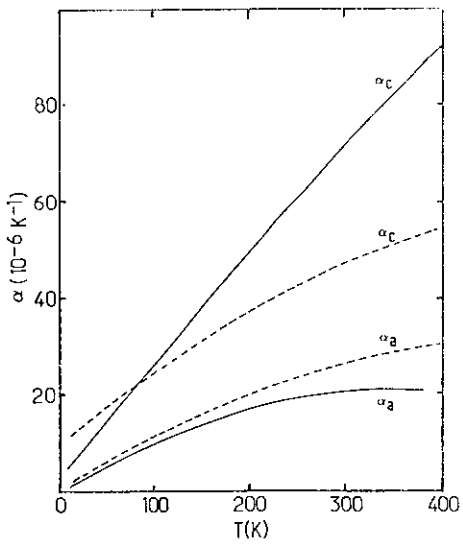

FIG. 2. Principal thermal expansion coefficients of $Li_{1-x}H_xIO_3$ vs. temperature. Dotted lines represent the same parameters for α-$LiIO_3$ (Ref. (*10*)).

of the principal thermal expansion coefficients) is of the same order of magnitude above RT for both compounds owing to a balancing effect originating in the opposite relative magnitude of the principal thermal expansion coefficients.

Atomic Coordinates

The variation of z(Li), z(O), and z(H) coordinates with temperature, of particular importance in interpreting the pyroelectric effect of $Li_{1-x}H_xIO_3$ (not yet measured to our knowledge), is shown in Fig. 3 in terms of atomic distances along the polar axis of the nearest atoms relatively to iodine in fixed location (z(I) = 0). As in α-$LiIO_3$, the spacing along the c axis of O with respect to I in the solid solution decreases when rising temperature (*11*). Owing to the error bars, the variation is considered as linear (rate -4×10^{-5} Å K^{-1}) over the whole temperature range. In contrast to α-$LiIO_3$,

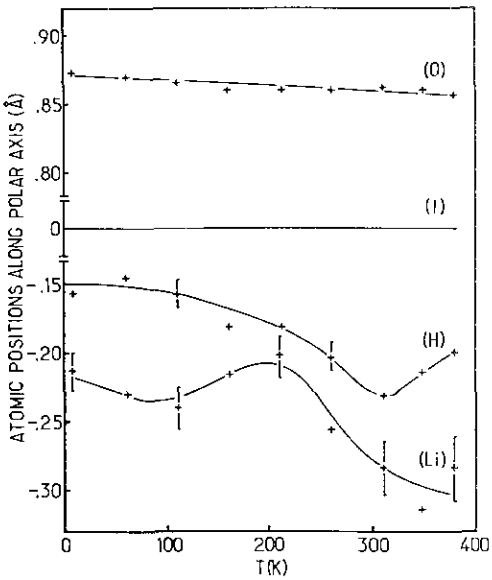

FIG. 3. Atomic positions (referred to iodine) along the polar axis of $Li_{1-x}H_xIO_3$ as a function of temperature. A few error bars corresponding to ±1 estimated standard deviation are given.

where the spacing of Li relative to I increases regularly according to a parabolic variation, in $Li_{1-x}H_xIO_3$ this spacing is almost a constant in the range 10–210 K, then increases drastically at the rate 55×10^{-5} Å K^{-1}. The relative distance of hydrogen increases regularly from 10 to 310 K, then decreases.

Bond Lengths and Atomic Coordination

Selected interatomic distances and angles are reported in Table III. The short I–O distance within the IO_3 pyramid is not corrected for thermal motion. The effect of this correction, assuming O riding on I, would be to reduce the apparent decrease of the I–O bond length upon increasing temperature and to yield a constant value of 1.808(1) Å over the whole temperature range (*11*). The ⟨O–I–O bond angle increases very slightly (13×10^{-4} ° K^{-1}) with rising temperature, this being due to the decrease of the oxygen–iodine spacing along the *c* axis, the I–O distances remaining constant. As in α-$LiIO_3$, the IO_3 group is rigid and its shape and dimensions are almost temperature independent. The I atom is also linked to three other O atoms. The long I—O bond of particular importance to verify the valence sum rule increases at a rate 15×10^{-5} Å K^{-1} between 100 and 350 K, whereas the ⟨O—I—O angle decreases (-22×10^{-4} °K^{-1}). It must be noted that the I—O distance in $Li_{1-x}H_xIO_3$ is shorter than in α-$LiIO_3$: 2.809 Å and 2.907 Å, respectively, at 295 K. This is related to the fact that the relative decrease of the *c* lattice parameter (4.4%) is larger than the increase of *a* (1.6%).

Lithium is octahedrally coordinated by oxygens. Within each LiO_6 coordination polyhedron the two sets of lithium–oxygen bond lengths (Li–O and Li—O) are not very well defined (esd's ≈ 0.01 Å), which reflects the small overall contribution of Li to the diffraction pattern as compared to the other atoms, and their variations are correlated to the shift of the *z*(Li) atomic displacement within the relatively rigid framework of IO_3 groups.

The hydrogen atom is located approximately along the line joining two oxygen atoms belonging to two different IO_3 groups, but is not exactly in the middle of this line. The ⟨O–H—O angle is practically constant (175°). The thermal evolution of the short O–H and long O—H distances consists in variations in opposite directions for the same reason as for the two types of lithium–oxygen distances. The general trend of the O–H—O bond is to become more and more symmetric from 10 to 300 K, then to restore its low temperature configuration in the range 310–380 K.

Amplitude of Thermal Vibration

The isotropic thermal parameter B_{iso} of hydrogen and the anisotropic temperature factor coefficients for Li, I, and O are reported in Table II as β_{ij} and correspond to the definition given in the table caption. These dimensionless β_{ij} elements are defined with respect to the oblique hexagonal

TABLE III

SELECTED INTERATOMIC DISTANCES (Å) AND ANGLES (°) IN $Li_{1-x}H_xIO_3$

T(K)	10	60	110	160	210	260	310	350	380
I–O	1.809(2)	1.808(2)	1.806(2)	1.803(2)	1.802(2)	1.803(2)	1.804(2)	1.804(2)	1.803(2)
⟨O–I–O	98.7	98.8	98.9	99.0	99.1	99.1	99.0	99.1	99.2
I—O	2.773(2)	2.775(2)	2.782(2)	2.789(2)	2.796(3)	2.803(3)	2.811(3)	2.818(3)	2.826(3)
⟨O—I—O	90.8	90.8	90.7	90.5	90.4	90.3	90.3	90.0	89.8
Li–O	2.070(8)	2.080(8)	2.084(8)	2.070(8)	2.064(8)	2.094(8)	2.110(10)	2.129(11)	2.111(14)
Li—O	2.232(9)	2.222(9)	2.220(9)	2.242(9)	2.257(9)	2.228(10)	2.217(12)	2.208(12)	2.232(15)
O–H	1.253(8)	1.244(8)	1.247(10)	1.278(8)	1.274(8)	1.303(8)	1.346(8)	1.283(11)	1.270(12)
O—H	1.767(8)	1.777(7)	1.778(9)	1.755(7)	1.763(7)	1.739(7)	1.702(7)	1.777(10)	1.797(10)
⟨O–H—O	176.4	176.8	175.6	173.2	174.7	176.4	176.1	173.8	172.9

crystal axis system. A local program based on the transformation given in Ref. (*12*) allows the conversion of the β matrix into a Cartesian system of axes. The solution of the eigenvalue problem of the latter matrix yields the mean-square displacements of atoms along the principal axes of the thermal ellipsoids and to the orientation of these axes relatively to any chosen direction. The mean-square amplitudes of vibration, averaged over all directions for each atom ($\langle u^2 \rangle_{\text{all dir.}}$), are shown in Fig. 4. They are defined as one-third of the sum of the eigenvalues of the matrix expressed in the Cartesian axes. This definition is used even when the thermal ellipsoid is significantly different from a sphere, i.e., even when the principal axes are different in length.

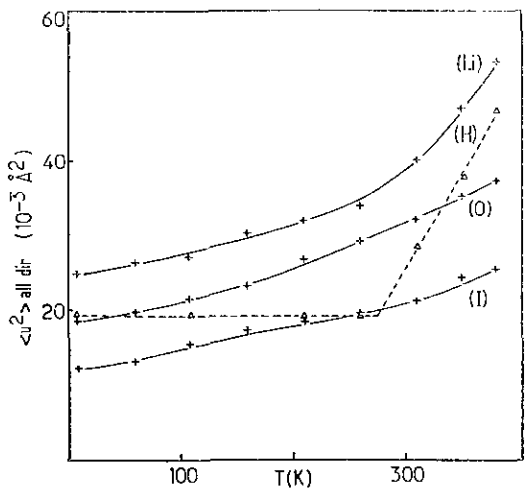

FIG. 4. Average isotropic mean square amplitudes of thermal vibration in $Li_{1-x}H_xIO_3$ as a function of temperature.

As expected, the mean square amplitude of vibration of the heavy iodine atom is the smallest among the four atoms and increases slightly with temperature ($\langle u^2 \rangle_{\text{all dir.}} = 21 \times 10^{-3}$ Å^2 at 295 K). Its thermal ellipsoid of revolution around the c axis is slightly elongated along this direction. The ratio of the lengths of the principal axes is 0.78 at 295 K and almost temperature independent.

The thermal ellipsoid of oxygen (the axes of which are significantly different at low temperature) is less elongated at high temperature; its shortest axis lies approximately along the short I–O bond. For this atom $\langle u^2 \rangle_{\text{all dir.}} = 31 \times 10^{-3}$ Å^2 at 295 K and the thermal evolution of this parameter is regular and similar to that of iodine.

The thermal ellipsoid of lithium is very elongated along the c axis; the ratio of the lengths of the principal axes is 0.38 at RT and nearly temperature independent. The mean square amplitude of vibration increases slowly from 10 K to about 250 K, then more rapidly ($\langle u^2 \rangle_{\text{all dir.}} \approx 39 \times 10^{-3}$ Å^2 at RT). It must be noted that $\langle u^2 \rangle_{\text{all dir.}}$ of I, O, and Li in $Li_{1-x}H_xIO_3$ are found to follow similar thermal behavior as in α-$LiIO_3$ (*11*) but with systematically larger values.

The mean-square amplitude of vibration ($B_{\text{iso}}/8\pi^2$) associated to the isotropic thermal parameter of hydrogen has the constant value 19(1) $\times 10^{-3}$ Å^2 between 10 and 260

K, then increases drastically up to 47(4) × 10^{-3} Å^2 at 380 K. This has to be related to the approach of the decomposition temperature (398 K) where protons begin to leave the lattice. Nevertheless it is surprising to find so small an amplitude of vibration at low temperature (about that of oxygen) for such a light atom; this point is discussed later.

Splitting of the Hydrogen Site?

In addition to the previously determined H site, a new site denoted by H′ in general position of $P6_3$ was included in the input list of the structure refinement program to take into account a possible split hydrogen site. For both hydrogen atoms a common isotropic temperature factor was fixed; each occupation factor was allowed to vary but the sum was constrained to the chemical composition $x = 0.34$. We choose to test the site H′ shown by stars in Fig. 5a, i.e., the site chemically similar to H, having the same z coordinate as H, but located between two other oxygens. Starting from approximate coordinates for this site, the refinement gives reliability factors similar to the case of a single hydrogen site; the H site coordinates as well as coordinates of other atoms retain the initial values within one esd, whereas the H′ position is shifted from the expected site, poorly defined (esd's of H′ coordinates are about 10 times esd's of H) and its occupancy is low (5 times lower than that of H). It can be concluded that the occurrence of another H′ site is highly questionable. It must be noted that the H and initial H′ sites are not crystallographically equivalent; in particular, their distances to the nearest iodine atoms are not the same owing to the rotation of IO_3 groups around the c axis (angle θ in Fig. 5b). This rotation of 17.9° at RT (15.2° in α-$LiIO_3$) away from the more symmetrical configuration corresponding to $\theta = 0$ explains that the six "vertical" edges of the oxygen octahedron around a given lithium site are not equivalent but split into two sets, although of same length.

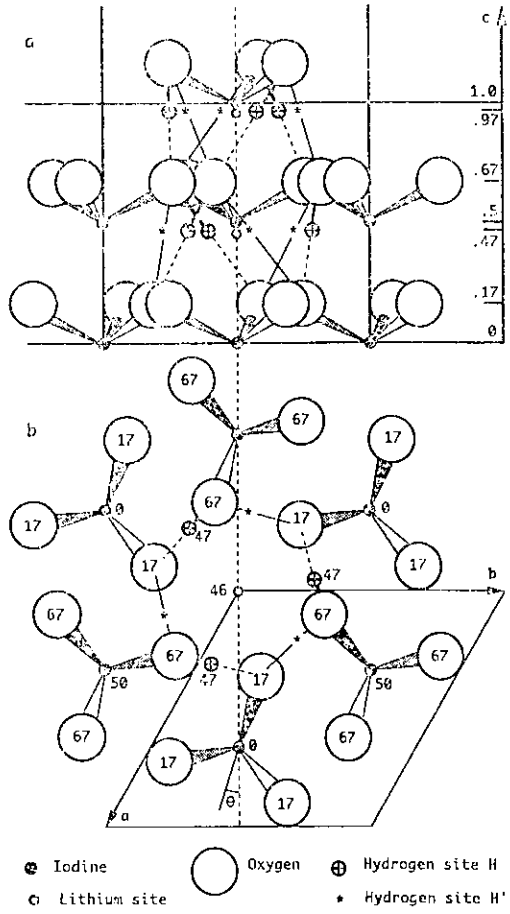

FIG. 5. Schematic representation of the structure of $Li_{1-x}H_xIO_3$. The numbers within or near the circles are the z reduced coordinates multiplied by 100 at 10 K. (a) Projection in a plane containing the c axis. Stars denote the tentative hydrogen sites H′ tested in the refinements. (b) The corresponding unit cell viewed along the c axis and showing the complete nearest environment of the lithium site.

Conclusion and Comments

High resolution neutron powder diffraction data, which give more accurate nuclear positional and mean-square displacement parameters than X-rays, particularly for light atoms in the presence of heavy atoms, have been used to investigate the thermal behavior of the structure of the $Li_{1-x}H_xIO_3$ solid solution.

A structural model taking into account a

split H site with a common isotropic temperature factor has been tested, but found to be inconsistent.

Structure refinements with an anisotropic temperature factor for hydrogen have been performed. Six β_{ij} coefficients were then refined for the hydrogen atom in general position and have been reported at room temperature in Ref. (*5*) for an equivalent H site. In this case the reliability factors are lowered by a nonsignificant amount in spite of the addition of five new parameters; this means that these new parameters are not statistically significant. Furthermore, when the esd's of β_{ij} are taken into account it is found that the precision of the thermal ellipsoid characteristics is poor and that one eigenvalue is always negative for $T \leq 260$ K. This eigenvalue is small compared to the two others; nevertheless, such a structural model also has to be turned down.

The small number of independent reflections (68) does not allow the use of a refinement program in which anharmonic thermal vibration factors are introduced. To get more reflections it would be necessary to grow a single crystal large enough for neutron diffraction, but up to now our attempts have always failed.

Nevertheless some clear structural features have been shown. The solid solution does not contain water molecules as previously mentioned by Hamid *et al.* (*7*). No first order phase transition occurs in the temperature range 10 to 380 K and the hexagonal space group $P6_3$ seems confirmed. Cell parameters increase regularly with rising temperature and the thermal expansion coefficient along the polar axis is much larger above 100 K than in α-$LiIO_3$. In $Li_{1-x}H_xIO_3$, lithium atoms occupy at random $(1 - x)$ of their α-$LiIO_3$ positions (Wyckoff site 2a), the probable location of protons corresponds to a random distribution in one type of general position (6c) with the occupation factor x. On the basis of Raman spectroscopy Barabash *et al.* (*13*) recently ascertained that the system behaves as a protonic glass. The presence of layers of statistically disordered protons between negatively charged laryers of IO_3 ions in planes perpendicular to the z axis is responsible for the shortening of the c lattice parameter as x increases. In addition, it is the source of a softer behavior than in α-$LiIO_3$ along the polar axis, as reflected by the thermal expansion coefficient, and is related to the more important response under stress; this must be of basic importance in interpreting the strong piezoelectric effect of this material.

We previously mentioned that the isotropic thermal parameter of hydrogen was abnormally small at low temperature. A possible interpretation, in connection with the failure of the refinement with an anisotropic temperature factor for H, would be the existence of two types of hydrogen atoms in the structure; the first type being bound, the second almost free in the lattice. Therefore only an average feature would be obtained from the refinements.

Disregarding hydrogen atoms, the main differences between α-$LiIO_3$ and $Li_{1-x}H_xIO_3$ in the thermal behavior of the structure are a shift above 210 K of the lithium position relative to the nearest layer of iodine atoms and a thermal ellipsoid of Li elongated along the c-axis, which are not observed in α-$LiIO_3$. The shift of the Li position (about 6×10^{-4} Å K^{-1} above 210 K) must induce large variations in the ionic contribution to the spontaneous polarization and so in the pyroelectric effect.

The quasi-one-dimensional ionic conductivity of α-$LiIO_3$ has been interpreted by considering two kinds of carriers (*14*): on one hand, interstitial Li ions hop among intersites in zigzag channels along the c axis and on the other hand, Li vacancies exchange positions with Li ions at lattice sites also along the c axis. Such a mechanism seems also suitable to interpret the electrical conduction of the solid solutions. Indeed, the larger the mole fraction x, the lower the conductivity (*7*). It is reasonable to assume that the presence of protons impedes the jumping of carriers within the zigzag chan-

nels. Furthermore, the occurrence of Li vacancies along the *c* axis, resulting from an occupation factor of the Li site smaller than unity, acts in favor of a predominating process of linear channels.

Finally, it must be noted that near room temperature and above, the structure of the solid solution appears to be strongly temperature sensitive, as evidenced by the thermal evolution of lithium and hydrogen parameters; this may be regarded as a disadvantage for technological applications under usual conditions.

Acknowledgments

We are grateful to B. Michaux (Dijon) for growing the sample.

References

1. J. E. Ricci and I. Amron, *J. Am. Chem. Soc.* **73,** 3613 (1951).
2. S. A. Hamid, *Phys. Status Solidi A* **43,** K29 (1977).
3. J. Bouillot, E. Coquet, J. Pannetier, and J.-M. Crettez, *Physica B* **136,** 493 (1986).
4. J.-M. Crettez, E. Coquet, B. Michaux, J. Pannetier, J. Bouillot, P. Orlans, A. Nonat, and J.-C. Mutin, *Physica B* **144,** 277 (1987).
5. J. Leroy, J.-M. Crettez, E. Coquet, and J. Bouillot, *Solid State Commun.* **75**(7), 539 (1990).
6. M. Remoissenet and J. Garandet, *Mater. Res. Bull.* **10,** 181 (1975).
7. S. A. Hamid, G. Kunze, and G. Reuter, *Acta Crystallogr. Sect. A* **33,** 261 (1977).
8. R. A. Young and D. B. Wiles, *J. Appl. Crystallogr.* **15,** 430 (1982).
9. A. W. Hewat, *Acta Crystallogr. Sect. A* **35,** 248 (1979).
10. E. Coquet, J.-M. Crettez, A. Bestaoui, J. Pannetier, and J. Bouillot, *Solid State Commun.* **63**(6), 557 (1987).
11. C. Svensson, J. Albertsson, R. Liminga, Å. Kvick, and S. C. Abrahams, *J. Chem. Phys.* **78**(12), 7343 (1983).
12. B. T. M. Willis and A. W. Pryor, "Thermal Vibrations in Crystallography," Chap. 4, Cambridge Univ. Press, London (1975).
13. A. I. Barabash, T. A. Gavrilko, A. M. Petrosyan, G. A. Puchkovskaya, and A. N. Roshchin, *Izv. Akad. Nauk. SSSR Ser. Fiz.* **55**(3), 515 (1991).
14. A. D. Zhang, S. F. Zhao, A. Y. Xie, and Z. Y. Xu, *Acta Phys. Sin.* **29,** 1158 (1980).